

## CHAPTER 5

# STELLAR POPULATION MODELS II: PERSISTENT STAR FORMATION AND A HOTTER IRS 16

G. H. Rieke & Peter Tamblyn

### Abstract

The compact cluster of luminous, blue stars imaged in Section 3.2 is distinct from the nuclear populations in M31 and M32. Steady-state models for the population are thus less likely to apply. A very recent burst of star formation such as discussed in Chapter 2 is a possible reconciliation of the cluster with these other galaxy nuclei. Stellar population models are now required to meet the considerably higher temperatures for the IRS 16-like stars determined from the properties observed in Chapter 3. A somewhat extended, but damped, star formation history comes closest to producing a population with the observed overabundance of very luminous, warm stars with the observed red stars. However, the comparison sample reviewed in Chapter 3 indicates that only a fraction of such stars would exhibit He I  $2.058 \mu\text{m}$  emission. The luminosities are also found to be almost unparalleled among warm Galactic stars. These problematic properties and the observed spatial distribution suggest that abnormal star formation or stellar evolution may be involved.

## 5.1 Introduction

The observations reported in Chapter 3 and contemporary observations (Libonate *et al.* 1995, Blum *et al.* 1995a, Blum *et al.* 1995b, Eckart *et al.* 1995, and Krabbe *et al.* 1995) clearly indicate that there is a large collection of He I emission stars in the central stellar cluster. The comparison sample presented in Section 3.3 finds close spectral analogues only among rare and mostly evolved massive stars. A comparison of this population with the nuclear populations in nearby galaxies and re-evaluation of stellar population models similar to those presented in Chapter 2 with this additional information are likely to provide considerable insight into the age or abnormality of the cluster.

## 5.2 Not Steady State

For comparison with the GC, we list properties of the nuclei of local group galaxies in Table 5.1. The black hole masses have been taken from Haller (1992), Lacy *et al.* (1991), Kormendy (1988), Lauer *et al.* (1992), and Richstone, Bower, & Dressler (1990) (we have assumed the value for M31 P1 to enhance its stability against tidal disruption); the core radii are from Rieke & Lebofsky (1987), Lauer *et al.* (1992), and Lauer *et al.* (1993). The absolute magnitudes at  $2.2\ \mu\text{m}$  have been interpolated from measurements available in the literature. To estimate upper limits to the central concentration of blue stars in the other galaxies, we have assumed that these stars have  $B - V$ ,  $V - R$ , and  $R - I$  colors of zero.

We have used the *HST/WFPC* measurements in Lauer *et al.* (1992) and Lauer *et al.* (1993) to estimate upper limits to the portion of the emission from the central 0.5 pc (diameter) that could arise from such stars, assuming that the remaining nuclear stellar population has colors identical to those observed just outside of the nucleus. In the case of M32, the Hopkins Ultraviolet Telescope data (O'Connell

Table 5.1: Nuclear Properties of Some Local Group Galaxies

| Galaxy    | $M_{BH}(10^6 M_\odot)$ | Core Radius (pc) | $M_K$ (10 pc)    | $M_{V \text{ or } B}$ (core) |
|-----------|------------------------|------------------|------------------|------------------------------|
| Milky Way | $\sim 2$               | $\lesssim 1.2$   | $-15.5$ to $-16$ | $\sim -10.3$                 |
| M31-P1    | $\sim 1(?)$            | 1.4              | —                | $> -4.9$                     |
| M31-P2    | $\sim 10$              | 3.7              | $-15.3$          | $> -5.1$                     |
| M32       | $\sim 3$               | cusped           | $-15.9$          | $> -4.9$                     |

*et al.* 1992) show the nucleus to be very red between 2500 and 1500 Å, so these data would yield a limit even more stringent than the one listed despite their relatively poor angular resolution. For the Milky Way, we have summed published fluxes (DePoy & Sharp 1991; Rieke *et al.* 1989) to get a total  $m_K = 7.5$  for the population of He I stars and assumed zero colors. The tabulated  $V$  or  $B$  magnitudes apply to the blue stellar component only, not to the integrated light from the nucleus. Although the nuclei of M31 (P1 and P2) and of M32 are very similar to that of the Milky Way in most respects, and bracket the properties of the Milky Way’s nucleus, it is noteworthy that any nuclear blue stellar cluster in these galaxies must be at least 100 times less luminous than in our galaxy.

### 5.3 Further Integrated Constraints

An additional set of constraints on the He I emitting stars can be derived from far-infrared mapping of the GC. Davidson *et al.* (1992) show that the far infrared is compatible with a centrally concentrated blue or ultraviolet source or sources with a luminosity of  $\sim 10^7 L_\odot$ ; luminosities as large as  $2 \times 10^7 L_\odot$  appear to contradict their data. In the following, we will define a “blue” source to be one capable of heating the dust in the region, while a “UV” source can both heat the dust and excite the gas. Since any hot stars are observed in the Rayleigh-Jeans portion of their spectrum, we can derive a simple relation between the integrated  $K$  magnitude in blue and

UV stars and their luminosity (approximating their outputs as blackbodies):

$$L \approx 10^{\frac{7.5-m_K}{2.5}} \left( \frac{T}{21,400 \text{ K}} \right)^3 \times 10^7 L_\odot. \quad (5.1)$$

We have assumed extinction at  $K$  equivalent to  $A_V = 30$  and the extinction law of Rieke & Lebofsky (1985). For example, if we assume the temperature of the UV sources is 33,000 K and that they have an integrated magnitude of  $m_K = 8.5$ , their luminosity would be  $1.5 \times 10^7 L_\odot$ , nearly violating the upper limit permitted by the far-infrared observations. However, we estimate the integrated  $K$  magnitude of the prominent hot sources to be  $m_K \sim 7.5$ , so most of these sources must have temperatures well below 33,000 K to satisfy the luminosity constraint. If we set the temperatures of these sources to 20,000 K, they have a luminosity of  $8 \times 10^6 L_\odot$ , and at this temperature they can contribute only a small portion of the UV. To stay within the luminosity limit, the source of the UV must then produce  $< 5 \times 10^6 L_\odot$ , requiring it to have an integrated  $m_K > 9.7$ . Perhaps one of the bright He I stars, or a number of faint ones, could be hot enough to provide the UV. However, the majority of the He I stars must have effective temperatures of roughly 20,000 K, similar to that modeled for the AF star by Najarro *et al.* (1994). Since it is improbable that the He I stars are significantly cooler than 20,000 K, from this calculation they do appear to provide the majority of the blue photons that are effective in heating the dust that produces the far-infrared emission, even if they do not dominate the excitation of the gas.

Along with the RSGs in this region, one expects a population of hot, main-sequence stars that is adequate to provide the UV (Rieke & Lebofsky 1982). The number of these stars can be estimated by Monte-Carlo population syntheses such as those of Chapter 2. These calculations suggest the presence of, on average, roughly 600 late O to early B main-sequence stars, which would be adequate to provide the  $10^{50}$  Lyman continuum photons required to excite the gas. The brightest of these

sources would be at  $m_K \sim 13$ . Although our observations leave open the possibility that the UV is provided by a minority of the He I stars, it appears more plausible that the gas is excited primarily by the hotter main-sequence stars in the young stellar population.

## 5.4 Additional Population Models

In Chapter 2, we used loose constraints on the properties of the “blue” luminous stars: they were required to match  $m_K$  within a factor of two, have  $T_{\text{eff}} > 5,000$  K, and the integrated population could not violate the UV or mass constraints. In light of the observations reported in Section 3.3, especially the comparison sample, it is tempting to place much more stringent constraints on matching the He I stars. However, we will first see that raising the minimum temperature is alone a very powerful constraint which is much less subject to remaining ambiguities of massive stellar evolution and  $K$ -band spectral properties. Morris *et al.* (1996) examines the  $K$ -band spectra of several “transitional” (OfI, Ofpe/WN9, WNL, B[e], and LBV) objects, a sample closely related to that presented in Section 3.3 despite a different motivation. They emphasize the sparse knowledge of these stars’ role in massive stellar evolution, inter-relations, and “peculiarity”. Specifically, “... peculiarity should *not* necessarily be implied in the formation and evolution of hot, massive stars that cannot (yet) be readily binned into a specific spectral subtype” [original emphasis and qualifier]. Although we believe that the broader samples in Hanson & Conti (1994) and Section 3.3 demonstrate the rarity of the combination of He I  $2.058 \mu\text{m}$  emission and extreme luminosity, we agree that it would be premature to declare that the GC stars are individually peculiar. Monte-Carlo synthesis models similar to those presented in Chapter 2 which do not depend on more subtle stellar characteristics than  $L$  and  $T_{\text{eff}}$  are ideally suited to exploring whether the *collection*

of warm, luminous stars at the GC is peculiar.

From a synthetic burst perspective, the most important result from our data is that many of the stars with  $m_K \leq 10$  are hotter than 15,000 K and hence more luminous than  $4.5 \times 10^5 L_\odot$ . Figure 5.1 is similar to Figure 2.1 but is based on newer tracks from the same group for  $Z=0.04$  with enhanced mass loss (Meynet *et al.* 1994) and the figure includes younger bursts which are now obviously required to meet the extreme luminosities of the GC stars. These newer tracks significantly reduce the impact of the UV characteristic temperature constraint because the most massive stars evolve to lower temperatures almost immediately. Figure 5.1 illustrates why, despite the reduced importance of the UV constraint, no single-burst models match all of the criteria in Table 2.1 and a minimum  $T_{\text{eff}}$  of 15,000 K for the IRS 16-like stars. Stars this luminous are present only at ages less than 5 Myr and, as stressed in Section 2.4, the RSG population is absent at these ages. Based on average quantities rather than randomly populated bursts, Krabbe *et al.* (1995) (K95) similarly exclude any single burst age unless RSGs are destroyed in preference to blue supergiants and AGB stars. Hence, we conclude that the GC population cannot be the result of a single, short star formation episode with a normal stellar distribution and normal stellar evolution.

However, the argument in Section 2.4.2 that a single burst must dominate the population needs to be reconsidered now that solo bursts are excluded. As proposed in that section, K95 find that a more complex star formation history can produce a more mixed population without violating the integrated constraints. They conclude that an earlier burst (Haller & Rieke 1989) produced RSG stars and a second, more persistent star formation episode, beginning 6–8 Myr ago with a decay time of 3–4 Myr, is responsible for  $\sim 30$  OBI and late-WR stars which are associated with the He I stars. Such models predict that the hottest, main-sequence stars in the

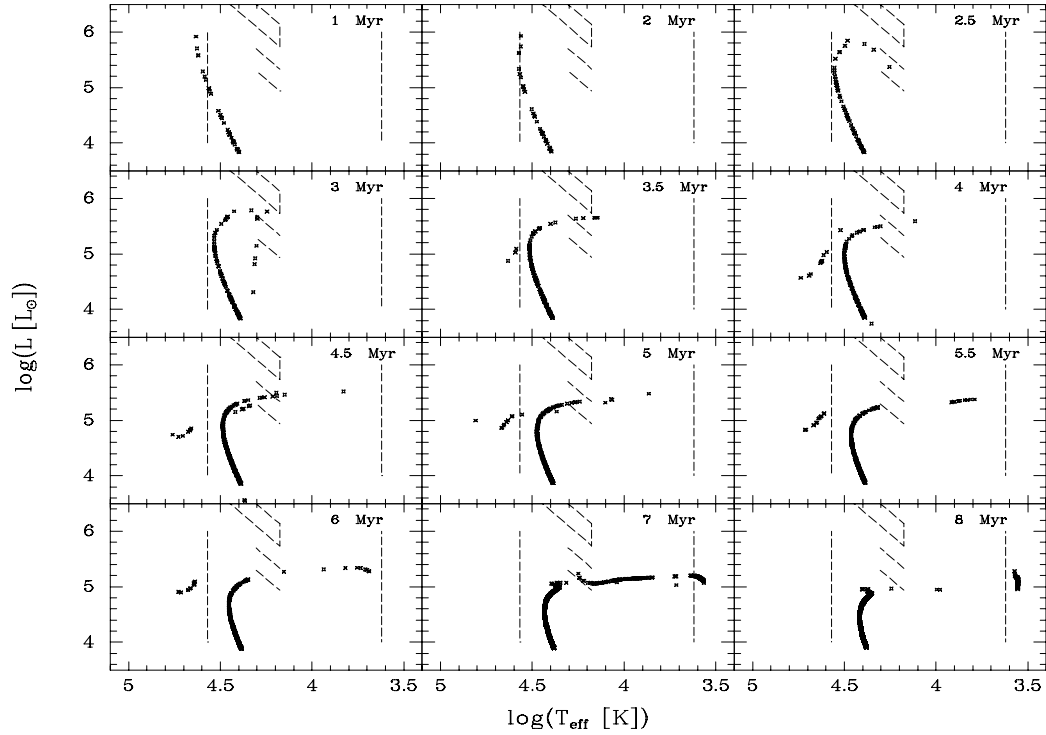


Figure 5.1: HR Diagrams of Bursts with Updated Tracks. The source tracks for these randomly populated bursts are from Meynet *et al.* (1994) for  $Z=0.04$  and enhanced mass loss. The dotted lines are at  $T_{\text{eff}} = 4, 170$  and  $37,000$  K as in Figure 2.1 and represent the regions of RSGs and the UV constraint. The rhombus is the location of the brighter He I sources with the cool edge at  $15,000$  K and top and bottom at  $m_K = 8.8$  and  $9.8$  ( $d = 8$  kpc,  $A_K = 3.47$ ). Line segments at  $m_K = 10.8$  and  $11.8$  (background) are also indicated for reference. Note that no stars are ever expected to match IRS 16NE well and that stars approach the region required to match IRS 16C, CC, NW, etc. only in bursts with ages  $\sim 3$  Myr but that RSGs do not develop for quite some time later. Also note the large number of O stars near the main sequence expected for young bursts and that they are fainter at  $K$  than the  $1''$  seeing background.



younger component dominate the UV instead of the He I emission stars. However, a smaller number of these hotter and more luminous stars is required in persistent formation models. We agree that such an exponentially decaying burst or a simpler two burst model with a much weaker second burst comes closer to meeting the burst criteria than a single burst. However, such models still do not predict the extreme luminosities, nor the ubiquitous presence of He I 2.058  $\mu\text{m}$  emission in the luminous, warm stars.

Further tests of this model of persistent star formation will become possible as imaging and spectroscopy with spatial resolutions substantially finer than 1'' become routine. With the reduced confusion such observations provide, it should be possible to identify the OV stars from a young burst. Although very little temperature information is available from NIR photometry of hot stars, they can be effectively distinguished from red giants. Averaged luminosity functions of bursts similar to those presented in Figure 5.1 are shown in Figure 5.2 with stars cooler than 4,170 K distinguished. These could be used to determine if a young burst with few OV stars or an older burst with many BV stars dominates the UV. Failure to detect many hot stars brighter than  $m_K \approx 14$  would indicate that the UV is dominated by very young stars (or a non-stellar source). This could also be tested with higher-resolution observations of the ionization state of the gas in the region. A UV-dominating young burst would have relatively few, dominant UV sources which might be discernable from ionization gradients. Eventually, high spatial resolution spectroscopy of the stars currently lost in the confusion may permit accurate determination of their spectral types in the manner of Hanson & Conti (1994).

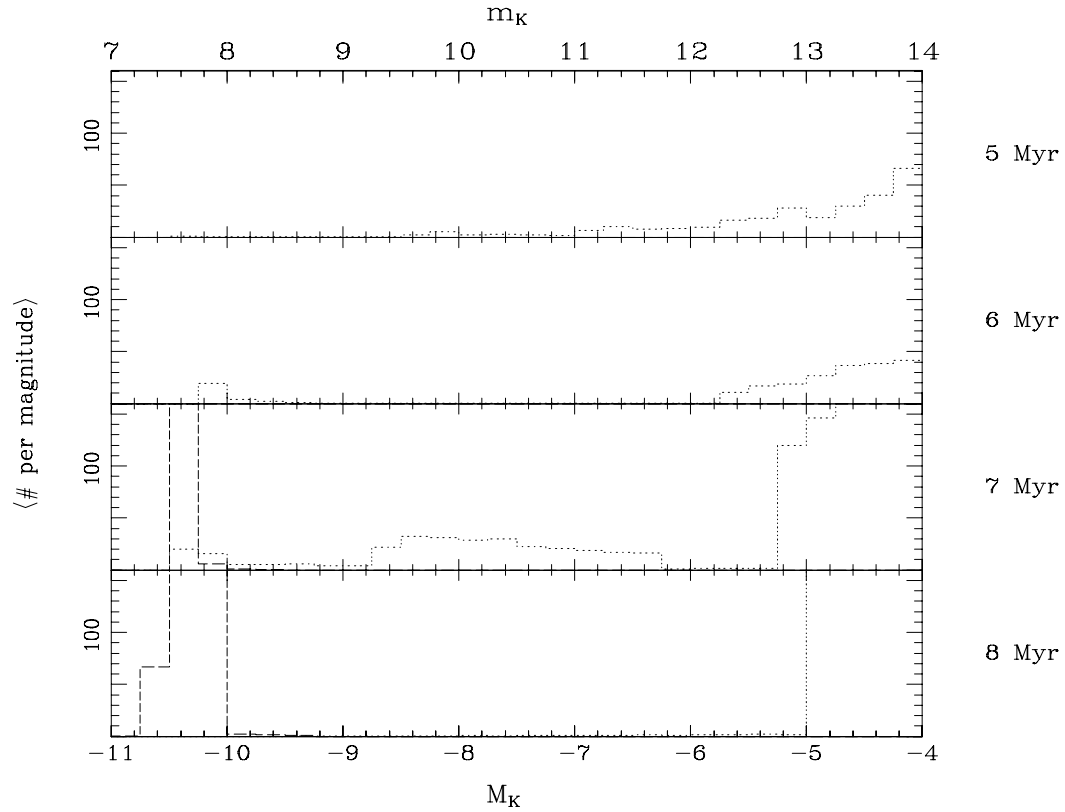


Figure 5.2: Predicted Luminosity Functions. The differential distribution of  $K$  magnitudes expected from UV-dominating bursts as in Figure 5.1 are plotted for stars hotter (dotted) and cooler (dashed) than 4,170 K. As higher-resolution observations of the region beat the confusion limit well below  $m_K \approx 12$ , the burst age may be discernable. The histograms for older bursts are truncated to emphasize expected dearth of intermediate brightness stars.

## 5.5 Line Emission and Luminosities

However, in evaluating the double (and extended) burst models we cannot ignore the results of Section 3.3 where we found that He I 2.058  $\mu\text{m}$  emission is an unusual trait, even among very luminous or windy late-O stars. Figure 5.3 compares the region of the HR diagram occupied by the IRS 16 components with many of the optically classified comparison stars. What is immediately apparent, despite the bias in the comparison sample towards luminous and peculiar stars and the uncertainty in the temperatures of the IRS 16 stars, is that they are almost unique in the Galaxy. Also, neither  $T_{\text{eff}}$  nor  $L$  alone is enough to separate the emission sources, contrary to the assumption required to model the GC population as evolved from a normal but persistent star formation event. Further, the criterion used to create this plot, that some He I emission is detectable in high-quality spectra, is much more generous than the criteria for detection of He I emission in the GC stars; fewer stars would have solid markers if subjected to equally stringent criteria. The comparison stars plotted are from Table 3.2, Hanson *et al.* (1996), McGregor *et al.* (1988b), and Morris *et al.* (1996). Those with ambiguous spectra have been excluded. The stellar parameters, listed in Table 5.2, are from an uncritical and incomplete review of the available literature and should not be over-interpreted. Figure 5.4 further emphasizes the paucity of stars analogous to the IRS 16 stars: only a few comparable stars are seen in a relatively complete sample of an entire galaxy (the LMC). Note that the HR diagram presented by Blum *et al.* (1995a) has the IRS 16 components  $\sim 1.7$  magnitudes fainter than in these two figures. Although they assume 0.5 magnitudes less extinction at  $K$ , this discrepancy arises primarily from their fit for  $BC_K$ , which is about 1.2 magnitudes below a blackbody; this is attributed to the infrared excesses in their comparison stars. The fit is pulled down by  $\eta$  Car, HR Car, and S Dor. We can exclude such a large IR excess for the bright GC sources because of their

Rayleigh-Jeans NIR colors. The fainter sources may well have significant IR excesses if they are related to these LBVs.

The luminosities of the bright GC emission-line sources are enough to determine that they must be massive, and hence uncommon. Although the remaining ambiguity in  $T_{\text{eff}}$  for these stars allows an order of magnitude uncertainty in  $L$ , they still must be exceptionally luminous. Given a luminosity, we can establish a minimum mass for the radiating object by comparing to the Eddington Luminosity,  $L_{\text{Edd}} = 4\pi GMcm_p/\sigma_T = 32,000 \frac{M}{M_\odot} L_\odot$ . This is the maximum luminosity an object with mass  $M$  can have in steady state because the opacity will always equal or exceed the Thompson opacity,  $\sigma_T$ . Applying this argument to IRS 16NE, which has  $L > 10^6 L_\odot$ , we derive a minimum mass over  $30 M_\odot$ . Although current data alone do not demonstrate that any of the other IRS 16 sources are quite this luminous, their masses must still be large. Further, a spread in effective temperatures is likely, and those which have higher temperatures than the minimum required to excite He I  $2.058 \mu\text{m}$  emission may also be more luminous than  $10^6 L_\odot$ .

## 5.6 Spatial Concentration

The various independent high-resolution  $2.058 \mu\text{m}$  emission images (Section 3.2; Eckart *et al.* 1995; Krabbe *et al.* 1995) also allow us to examine the spatial distribution of He I emitting stars. The original, larger scale image (Krabbe *et al.* 1991) combined with these new images of the central cluster show that the He I stars, especially the bright ones, are much more centrally concentrated than the stars (compare to continuum images such as in Eckart *et al.* 1993). A similar gradient in the WR fraction is seen in the dense core of the giant H II region NGC 3603 (Moffat *et al.* 1985). The crossing time of the central  $1/4$  pc of the GC at typical stellar velocities is only 1000 yr, hence the population should be well mixed on a

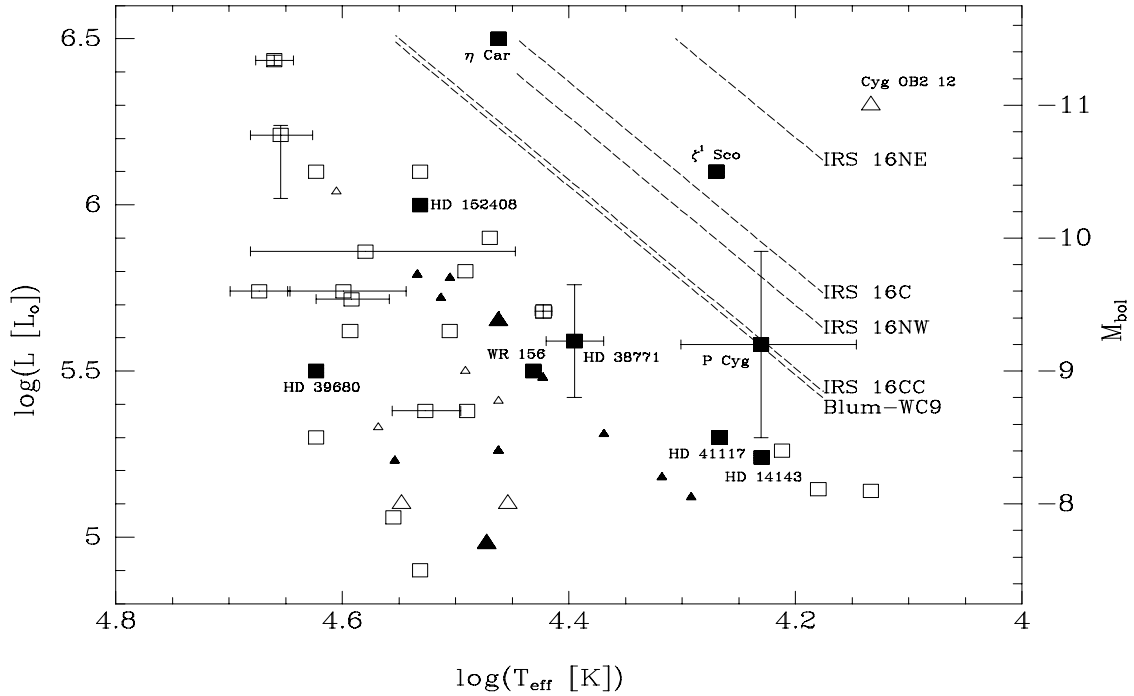


Figure 5.3: Luminous Galactic Emission-Line Stars Compared to the IRS 16 Sources. Filled symbols are comparison stars with the He I  $2.058 \mu\text{m}$  emission line; open symbols are stars without the line or with only absorption in the line. Squares are used when both  $T_{\text{eff}}$  and  $L$  are available from the literature; small triangles are used when both had to be estimated from spectral type (Schmidt–Kaler 1982); large triangles are used when one had to be estimated. Error bars are indicated where available or where the literature has discordant values. The IRS 16 luminosities assume blackbodies at a distance of 8 kpc with  $A_K = 3.47$ . The extraordinary luminosities of the IRS 16 components are the most striking features.  $\eta$  Car,  $\zeta^1$  Sco and Cyg OB2 12 are known to be atypical stars. The figure also demonstrates that neither extreme luminosity nor  $T_{\text{eff}}$  alone determines the trait of He I  $2.058 \mu\text{m}$  emission.

Table 5.2: Parameters of Selected Comparison Stars

| Name          | Spectral Type | $\log(T_{\text{eff}} [\text{K}])$ | $\log(L [L_{\odot}])$ | He I ? |
|---------------|---------------|-----------------------------------|-----------------------|--------|
| Cyg OB2 12    | B5Ia          | 4.13                              | 6.3                   | n      |
| HD 36371      | B4Ia          | 4.13                              | 5.14                  | n      |
| HD 14134      | B3Ia          | 4.18                              | 5.14                  | n      |
| HD 75149      | B3Ia          | 4.21                              | 5.26                  | n      |
| HD 183261     | B3II          | 4.22                              | 4.61                  | n      |
| HD 14143      | B2Ia          | 4.23                              | 5.24                  | y      |
| HD 209008     | B3III         | 4.23                              | 3.74                  | n      |
| P Cyg         | B2pe/LBV      | 4.23                              | 5.58                  | y      |
| $\zeta^1$ Sco | B1.5Ia+       | 4.27                              | 6.1                   | y      |
| HD 41117      | B2Iaevar      | 4.27                              | 5.30                  | y      |
| HD 207329     | B1.5Ib:e      | 4.29                              | 5.12                  | y      |
| HD 2905       | B1Iae         | 4.32                              | 5.18                  | y      |
| HD 185859     | B0.5Iae       | 4.37                              | 5.31                  | y      |
| HD 38771      | B0Iab:        | 4.40                              | 5.59                  | y      |
| BD+36 4063    | ON9.7Ia       | 4.42                              | 5.48                  | y      |
| HD 191781     | ON9.7Ib       | 4.42                              | 5.48                  | y      |
| HD 37128      | B0Iab:        | 4.42                              | 5.68                  | n      |
| WR 156        | WN8           | 4.43                              | 5.5                   | y      |
| HD 191765     | WN6           | 4.45                              | 5.10                  | n      |
| AS 268        | WN8           | 4.46                              | 5.26                  | y      |
| AS 306        | WN8           | 4.46                              | 5.65                  | y      |
| BD+59 2786    | B0III         | 4.46                              | 5.41                  | n      |
| HD 177230     | WN8           | 4.46                              | 5.26                  | y      |
| $\eta$ Car    | LBV           | 4.46                              | 6.5                   | y      |
| HD 313846     | WN9           | 4.47                              | 5.9                   | n      |
| HD 50896      | WN5           | 4.47                              | 4.98                  | y      |
| HD 209975     | O9.5Ib        | 4.49                              | 5.38                  | n      |
| SAO 20924     | B0III/O9e     | 4.49                              | 5.5                   | n      |
| WR 22         | WN7           | 4.49                              | 5.8                   | n      |
| HD 210809     | O9Ib          | 4.50                              | 5.62                  | n      |
| Roberts 89    | WN7           | 4.50                              | 5.78                  | y      |
| X Per         | O9pe          | 4.51                              | 5.72                  | y      |
| HD 151804     | O8Iaf         | 4.53                              | 6.1                   | n      |
| HD 152408     | O8:Iafpe      | 4.53                              | 6.0                   | y      |
| HD 193322     | O9V((n))      | 4.53                              | 4.9                   | n      |
| HD 225160     | O8e           | 4.53                              | 5.79                  | n      |
| HD 36861      | O8III(f)      | 4.53                              | 5.38                  | n      |
| MWC 627       | O8e           | 4.53                              | 5.79                  | y      |
| HD 192163     | WN6           | 4.55                              | 5.10                  | n      |
| HD 60848      | O8V:pevar     | 4.55                              | 5.23                  | y      |
| HD 214680     | O9V           | 4.56                              | 5.06                  | n      |
| HD 194334     | O7.5Ve        | 4.57                              | 5.33                  | n      |
| HD 14947      | O5.5f         | 4.58                              | 5.86                  | n      |
| HD 190864     | O6.5III(f)    | 4.59                              | 5.62                  | n      |
| HD 206267     | O6V           | 4.59                              | 5.72                  | n      |
| HD 229232     | O5e           | 4.60                              | 6.04                  | n      |
| HD 46150      | O5V((f))      | 4.60                              | 5.74                  | n      |
| HD 190429     | O4.5If+       | 4.62                              | 6.1                   | n      |
| HD 199579     | O6V           | 4.62                              | 5.3                   | n      |
| HD 39680      | O6:pe         | 4.62                              | 5.5                   | y      |
| HD 15558      | O5.5III(f)    | 4.65                              | 6.21                  | n      |
| HD 15570      | O4If+         | 4.66                              | 6.44                  | n      |
| HD 15629      | O5V((f))      | 4.67                              | 5.74                  | n      |

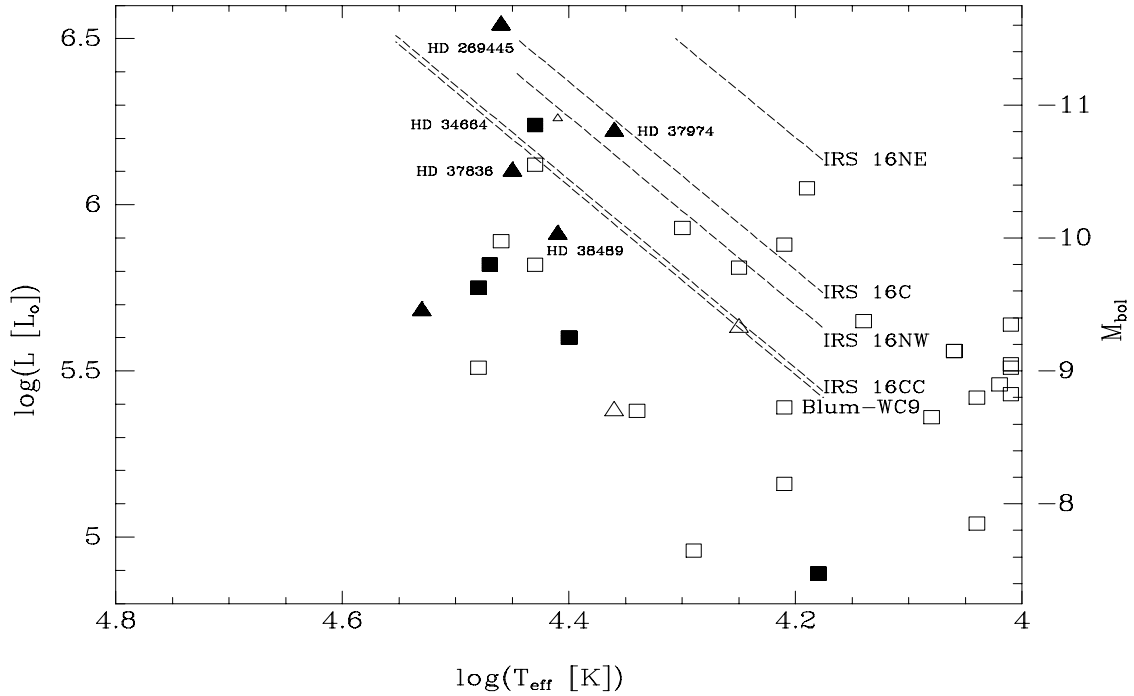


Figure 5.4: Luminous Stars in the Large Magellanic Cloud Compared to the IRS 16 Sources. As in Figure 5.3, filled symbols represent stars with the He I  $2.058\mu\text{m}$  emission line and open symbols represent stars without this emission line; squares are used for stars with well determined parameters while triangles or small triangles are used for stars with inconsistent colors. The LMC stellar parameters are from McGregor *et al.* (1988a); the luminosities of GC sources assume blackbodies at a distance of 8 kpc with  $A_K = 3.47$ . Note that even in a relatively complete sample of a galaxy's stars, only a few appear to be like the IRS 16 stars. This comparison also suggests somewhat hotter temperatures, near 25,000 K, for the emission stars, and consequently luminosities well above  $10^6 L_\odot$ .

much larger scale. As the observed stellar properties are not well mixed, a second influence is required. The cluster relaxation timescale is of order 80 Myr (Lee 1993), hence the young stars are not mass segregated. A possibility is that the outer- and inner-most He I stars are not co-eval but from distinct bursts. In this picture, the RSGs and outer WR stars are slightly older. This is consistent with the population models which predict that older He I stars should be fainter: it is now recognized that the He I sources associated with IRS 9, 11, and 15 are not dominant continuum sources. One would also expect a correlation of line width with spatial location in the cluster if an earlier burst is less centrally concentrated. The older, wide-lined WRs would be typically observed with a larger projected separation from the cluster center. Figure 5.5 illustrates that this correlation is exhibited in the GC. However, this figure is constructed from data which have a selection bias towards finding large equivalent width and hence preferentially wide-lined stars at larger projected distances. If the young GC stars formed in two bursts, it is not obvious why the stars from a second burst would be trapped further down in the central potential. Another possibility is that some property of the central 1/4 pc enhances the proportion of sources with He I emission. This possibility will be examined in the next chapter.

## 5.7 Summary

The GC blue stellar population has an integrated  $m_B \approx 7.5$ ; comparison with *HST* data on M31 and M32 indicates that the GC is either unique in some unknown way or not in a steady state. The observational demonstration that the bright blue GC stars are mostly He I emission sources and hence have  $T_{\text{eff}} \gtrsim 15,000$  K also allows a more detailed examination of the complex star formation history scenario discussed in Section 2.4. New tracks from the same source as the tracks used in Chapter 2 significantly reduce the impact of the UV characteristic temperature con-



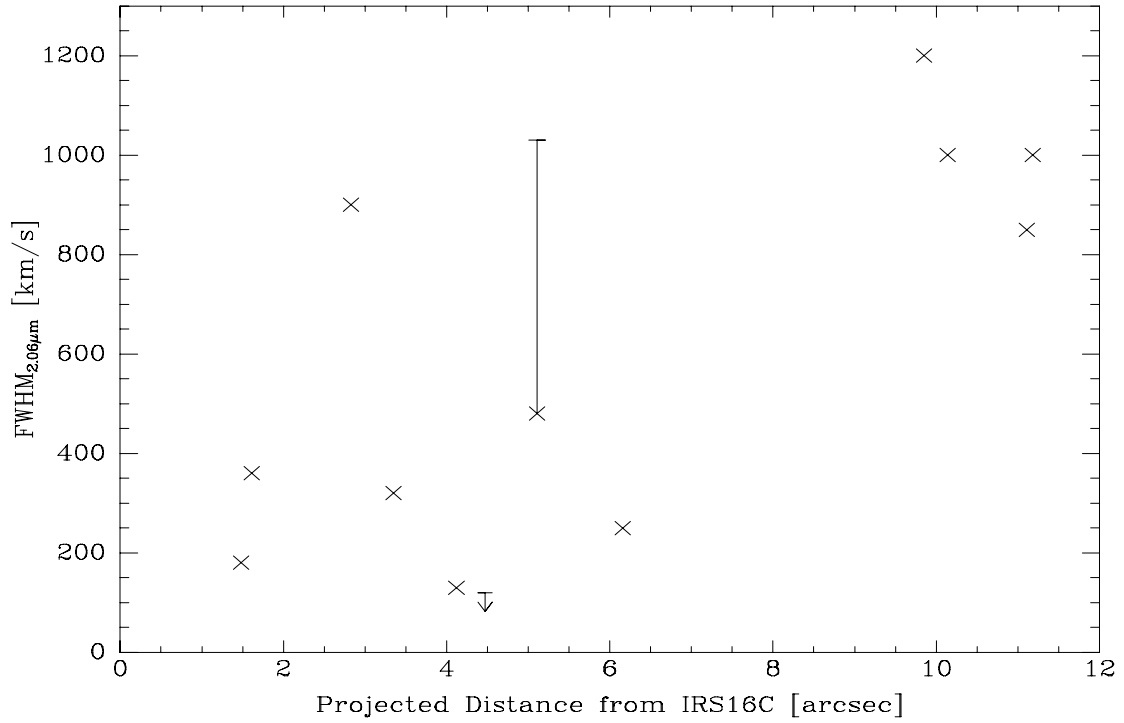


Figure 5.5: Correlation of Line Width with Projected Distance. The width (FWHM) of the He I  $2.058\ \mu\text{m}$  emission line is apparently correlated with projected distance from the center of the stellar cluster (near IRS 16C). This correlation is consistent with the two burst hypothesis. The projected distances are from Table 3.4; the line widths are from Table 3.3 and Najarro *et al.* (1994). The large error bar for IRS 13 reflects the FWHM measured by Blum *et al.* (1995a) from high quality data; we also saw a broad line base which we excluded from the profile fit.

straint but continue to have difficulty reproducing stars as luminous as IRS 16NE. Population models which make a large allowance for uncertainty in massive stellar evolution indicate that a persistent or episodic star formation history might be able to reproduce the GC stellar population without invoking unusual star formation or evolution. However, comparison with luminous Galactic emission-line stars demonstrates that the GC stars are nearly unique and hence cannot arise in such numbers from normal stellar evolution. The concentration of bright He I sources to the central  $1/4$  pc may hint to their origin.